Structural Changes in the Melt Spinning, Cold Drawing, and Annealing of Poly(4-methylpentene-1) Fibers

Cheol-Ho Choi, James L. White

Institute of Polymer Engineering, University of Akron, Akron, Ohio 44325

Received 10 October 2003; accepted 27 May 2004
DOI 10.1002/app.21929
Published online in Wiley InterScience (www.interscience.wiley.com).

ABSTRACT: Isotactic poly(4-methylpentene-1) melt-spun fibers were investigated. Prior investigators of melt-spun fibers found that these fibers have a tetragonal unit cell (Form I). We obtained the same unit cell structure in melt-spun fibers. We found that higher draw-down-ratio fibers had *d*-spacings closer to the previously cited values of Form I. We also found that cold-drawn fibers had similar values to those of melt-spun fibers. However, after these were annealed at 200°C, the unit cell was changed. It is possible that this new unit cell was the orthorhombic form of He and Porter. We also observed the birefringence of these fibers. The values changed after the melt-spun fibers were cold drawn and annealed. The melt-spun fiber values reached 0.006. The values for the drawn fibers were as high as 0.007. We suggest that the intrinsic birefringence is about 0.0075. © 2005 Wiley Periodicals, Inc. J Appl Polym Sci 98: 130–137, 2005

Key words: annealing; polyolefin; isotactic

INTRODUCTION

Isotactic poly(4-methylpentene-1) (P4MP1) first described by Natta et al.[1,2] P4MP1 has, through the years, been variously studied as an injection-molding resin,[3–5] a fiber,[6,7] and a film.[8,9] Various researchers[4–10] have performed structural studies on these products.

In this article, we describe the melt spinning and subsequent solid-state drawing and annealing of fibers and the associated structural changes.

Background

Detailed studies of isotactic P4MP1 crystal structure have been made by various researchers (Table I), beginning with Frank et al.[11] These authors found a tetragonal unit cell based on 7/2 helices with dimensions of $a = b = 18.66$ and $c = 13.80$ Å. Litt[12] and Kusanagi et al.,[13] who studied melt-drawn samples, derived similar unit cells (Table I). This unit cell was called form I.

There have been various studies on the influence of solvents on P4MP1 crystallization.[14–23] These investigations have involved the swelling of form I with organic liquids and the precipitation of crystals out of solution. Various new crystalline unit cells have been found (Table I). Form II, which has 4/1 helices, is tetragonal and is obtained from dilute xylene solutions.[14–16] Form III also has 4/1 helices in a tetragonal unit cell.[21] Form IV has 3/1 helices and a hexagonal crystal structure.[22]

He and Porter[23] studied the uniaxial drawing of P4MP1 by solid-state coextrusion at 150°C. The products were characterized with wide-angle X-ray diffraction and differential scanning calorimetry. They found that the crystal structure was a new tetragonal form ($a = b = 18.35$ Å and $c = 13.52$ Å) at lower draw ratios (DRs). At higher DRs, it was orthorhombic ($a = 17.70$ Å, $b = 8.85$ Å, and $c = 12.33$ Å). They found that the crystallinity of drawn P4MP1 increased up to about 90%.

Isotactic P4MP1 has been prepared in the form of single crystals[11,17,24] and, when crystallized in the quiescent state, exhibits spherulitic structures.[25,26] This makes it a well-behaved crystalline polyolefin. It has the peculiar features of having an amorphous density very close to its crystalline density, which allows it to be transparent, and a β transition just below room temperature.

The melt spinning of isotactic P4MP1 fibers has been considered by Noether and Whitney[6] and ourselves.[7] It has been found the P4MP1 fibers were Form I.

EXPERIMENTAL

Materials

The isotactic P4MP1 in this study was the same as that described in our earlier article.[7] It was MX002 from Mitsui Chemical Co.: melting temperature (T_m) = 235°C, melt flow rate = 22, dielectric constant = 2.12 (at l00–1 MHz), transparency = 91%, and density = 0.835 g/cm^3.

Correspondence to: J. L. White.

TABLE I
Prior Investigations of Crystal Structure

Form	Helix	Unit cell geometry	*a* (Å)	*b* (Å)	*c* (Å)	Authors	Remarks
I	7/2	Tetragonal	18.66	18.66	13.80	Frank et al.[11]	Single crystal precipitated from xylene
	7/2	Tetragonal	18.50	18.50	13.76	Litt[12]	Melt-drawn
	7/2	Tetragonal	18.70	18.70	13.68	Kusanagi et al.[13]	Stretch-quenched amorphous strip at 95°C annealed at 230°C
II	4/1	Tetragonal	19.16	19.16	7.12	Takayanagi and Kawasaki[15]	Hot xylene solution into a water bath at 25°C
						DeRosa[16]	
	4/1	Monoclinic	10.49	18.89	7.13	Charlet and Delmas[18–20]	Precipitated from tetramethyl tin solution
III	4/1	Tetragonal	19.38	19.38	6.98	Charlet and Delmas[18] and DeRosa[22]	Precipitated from xylene cyclohexane solutions
IV	3/1	Hexagonal	22.17	22.17	6.5		Crystallization of cyclopentene solutions

Melt spinning

P4MP1 was melt spun from the barrel of an Instron capillary rheometer with a capillary spinneret with a diameter of 1.6 mm and length-to-diameter ratio of 9.3 (Fig. 1). The throughput rate was 0.54 cm^3/min. A T_m of 270°C was used. Filaments with draw-down ratios (DDRs) of up to 300 were produced. A Rothschild electronic tensiometer was used to obtained spinline tensions (F_L's) and stresses ($4F_L/\pi d^2$, where d is the filament diameter).

Drawing and annealing

The melt-spun fibers were drawn with the Instron tensile tester (10 mm/min) at room temperature. The highest DR obtained was near 3.

The P4MP1 melt-spun fibers were subsequently set on a metal holder, which was inserted into an oven for heat treatment under various conditions. These filaments were essentially annealed under tension.

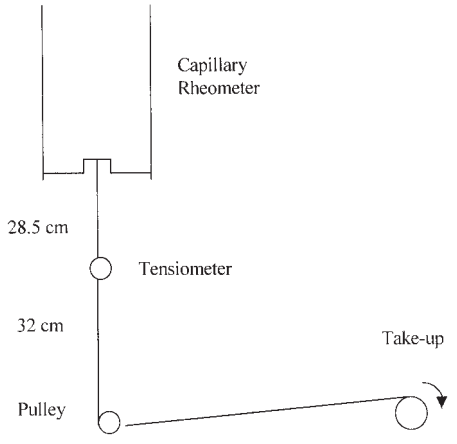

Figure 1 Melt-spinning apparatus.

Characterization

The P4MP1 melt-spun fibers were characterized by wide-angle X-ray diffraction with a Bruker X-ray device equipped with a copper target tube, and a graphite crystal monochrometer was used to obtain Cu Kα radiation (λ = 1.5418 Å). X-ray diffraction was applied to determine the crystal structure.

The birefringence of the fibers was measured with a Leitz polarized light microscope with a Berek compensator.

We determined the Hermans–Stein orientation factors $f_2(j = a, b, c)$:[27]

$$f_j = \frac{3\cos^2\phi_j - 1}{2} \quad (1)$$

where j refers to the crystallographic axis and ϕ_j is the angle between the j crystallographic axis and the fiber axis for the melt-spun and melt-drawn fibers. The form I tetragonal unit cell, as described in our previous article,[7] was used to interpret orientation. The (200) wide-angle X-ray scattering (WAXS) reflection was used in our calculations.

RESULTS

A typical WAXS diffractometer scan for a melt-spun P4MP1 filament is shown in Figure 2. The sample showed a high level of crystalline orientation. We summarize the observed 2θ and d-spacings in Table II.

We studied the orientation of the melt-spun fibers from WAXS patterns. The Hermans–Stein orientation

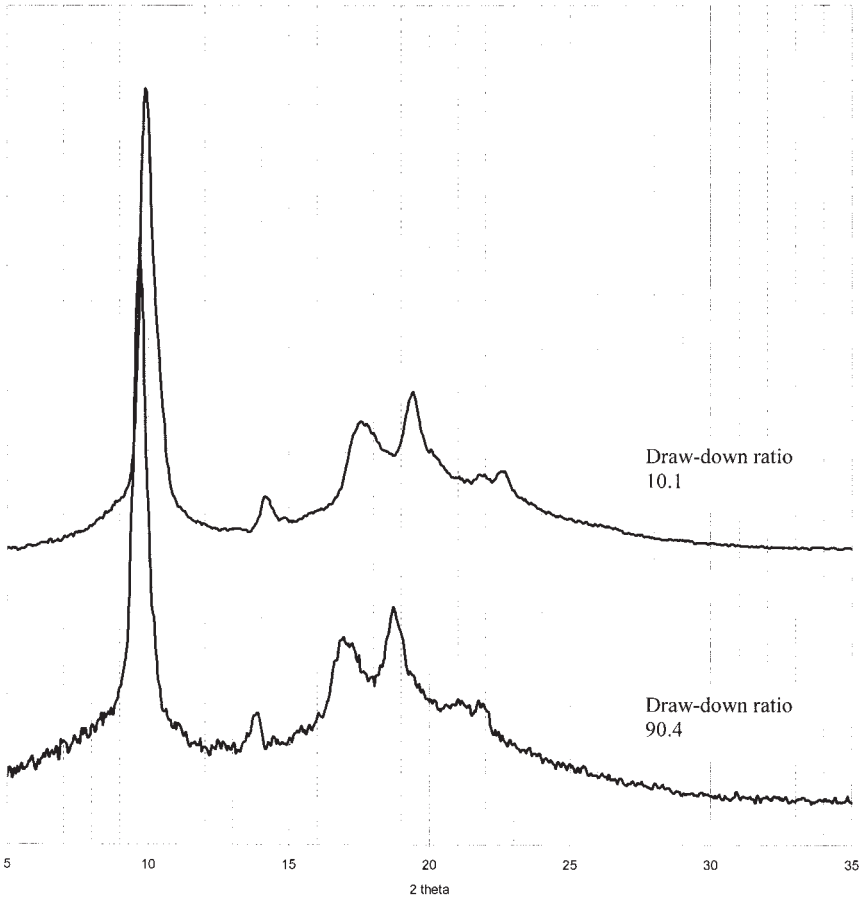

Figure 2 Typical equatorial WAXS diffractometer scans of the melt-spun fibers of P4MP1 produced at various DDRs.

factors are shown as a function of spinline stress in Figure 3. The birefringence is similarly plotted in Figure 4. The crystalline orientation factors were rather high for melt-spun fibers, the birefringences' rather low f_c reached about 0.85, and the birefringence was 0.006.

We subsequently subjected the fibers to cold drawing. In Figure 5, we show typical engineering stress–strain curves for the P4MP1 filaments. These indicated neck development and strain hardening.

In Figure 6(a,b), we show a WAXS diffractometer scan of a typical cold-drawn fiber. We summarize the *d*-spacings for the drawn fibers in Table III. The WAXS pattern shows a very high level of crystalline orientation. A chain-axis crystalline orientation factor of 0.95 was determined. The birefringence of the fiber was increased to 0.007.

The melt-spun and cold-drawn fibers were both annealed at 200°C. Typical WAXS patterns for the annealed fibers are shown in Figure 7. The *d*-spacings are given in Tables IV and V.

TABLE II
$2\theta_{obs}$ Angles and *d* Spacings for Melt-Spun P4MP1 Fibers as a Function of DDR

DDR = 10.1		DDR = 90.4	
$2\theta_{obs}$	*d*-spacing	$2\theta_{obs}$	*d*-spacing
9.9	8.93	9.7	9.12
14.2	6.24	13.8	6.42
17.6	5.04	17.0	5.22
19.4	4.58	18.8	4.72
21.9	4.06	21.1	4.21
22.6	3.93	21.9	4.06

INTERPRETATION

d-spacings and unit cells

Table I summarizes the observed *d*-spacings for the melt-spun fibers. Although the same number of closely related *d*-spacings existed for all of the fibers, the values of the *d*-spacings steadily increased about 0.13 to 0.20 Å as the spinline stress increased. The higher DDR fibers had *d*-spacings closer to the values of Frank et a1.,[11] Litt,[12] and Kusanagi et a1.[13] (see Table VI).

Table II summarizes the *d*-spacings for the cold-drawn P4MP1 fibers. The values did not change from those of the melt-spun fibers.

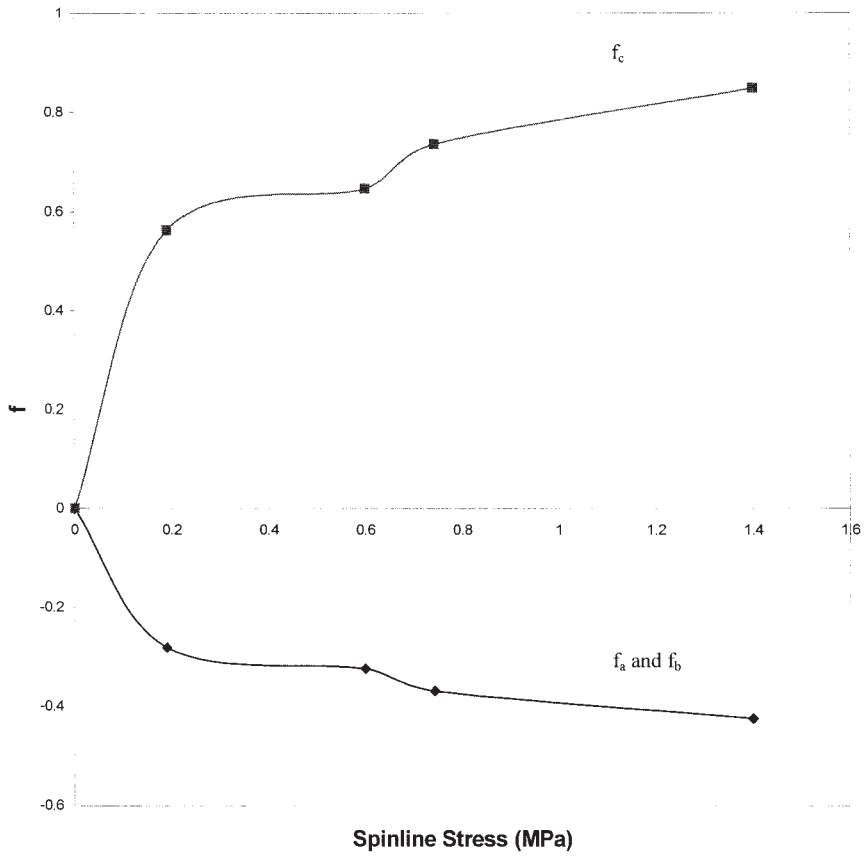

Figure 3 Hermans–Stein orientation factors f_a, f_b, and f_c for the P4MP1 fibers as a function of spinline stress.

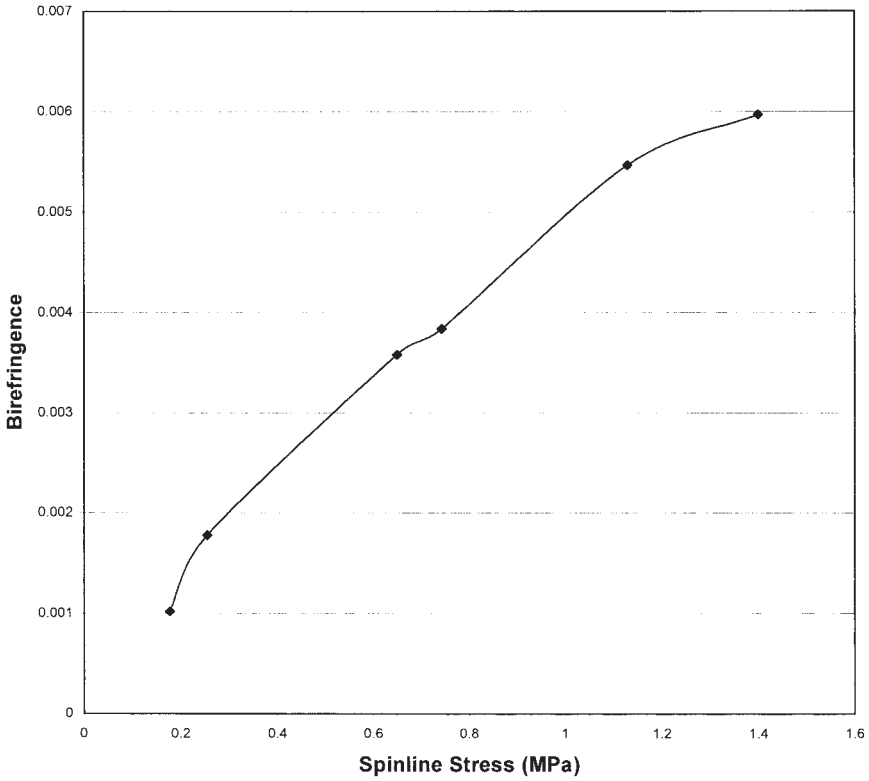

Figure 4 Birefringence of P4MP1 melt-spun fibers as a function of spinline stress.

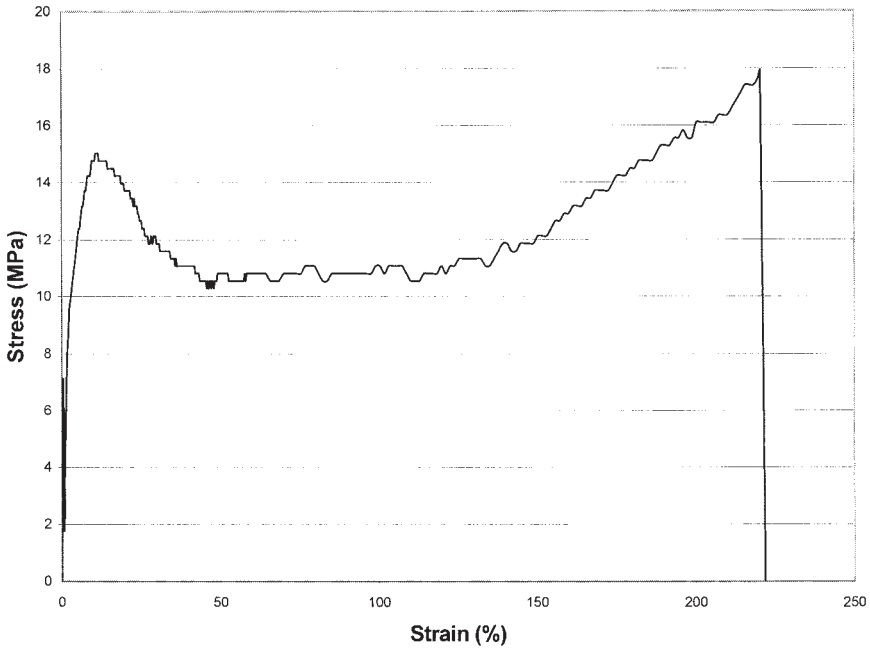

Figure 5 Engineering stress–strain curve during the cold drawing of the P4MP1 filament.

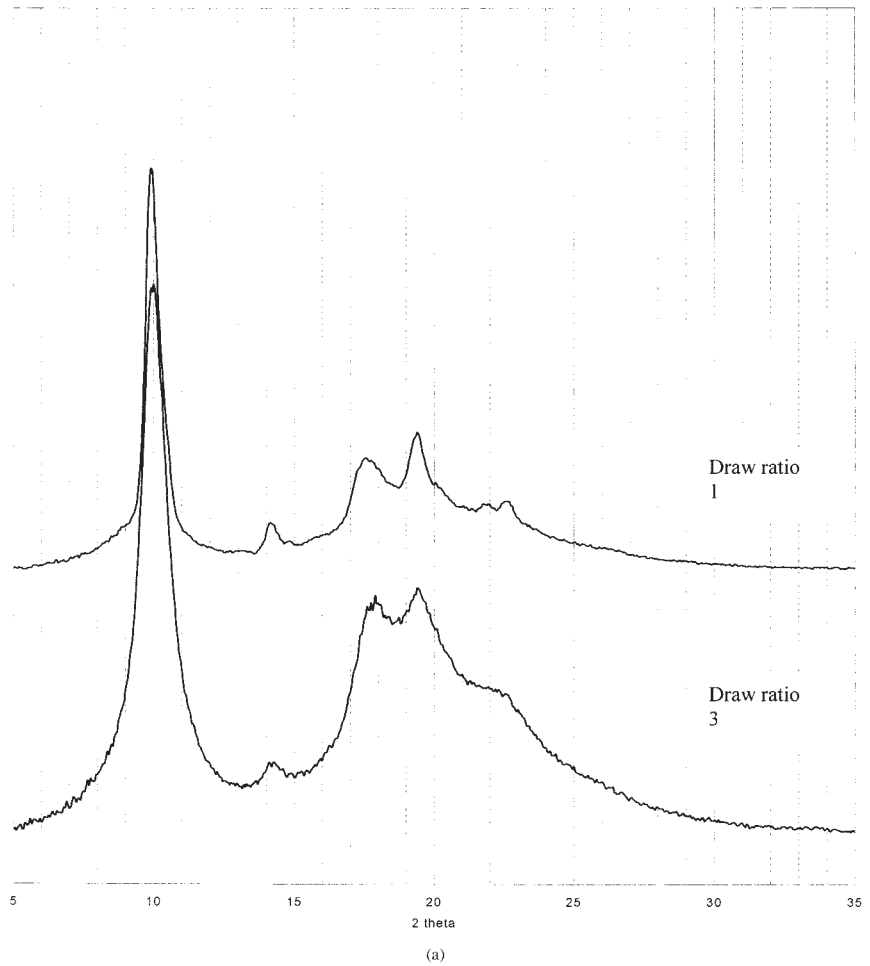

Figure 6 X-ray diffractometer scan of cold-drawn fibers of P4MP1: melt-spinning DDR = (a) 10.1 and (b) 90.4.

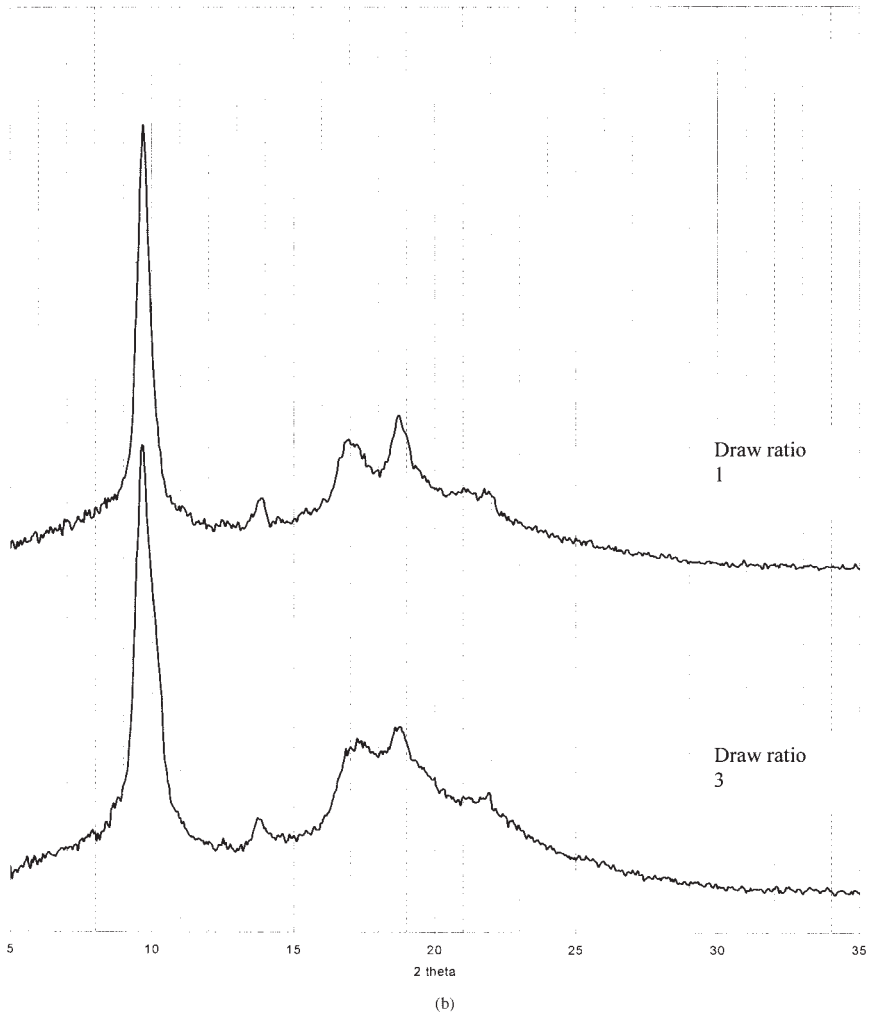

Figure 6 (*Continued from the previous page***)**

The *d*-spacings for the annealed fibers are contained in Tables IV and V. The values for the annealed and drawn/annealed fibers were reduced on the order 0.15 to 0.4 Å from those of the melt-spun fibers. The values of the *d*-spacings were also much lower than those predicted by the unit cells of Frank et a1.,[11] Litt,[12] and Kusanagi et a1.[13]

The shifts in the *d*-spacings of the annealed fibers were similar to those reported by He and Porter[22] for solid-state extruded samples. They suggested an orthorhombic unit cell to correlate with their *d*-spacings. In Table VII, we compare the He–Porter predictions with our observations.

Birefringence

The highest birefringence found with the melt-spun fibers was 0.006. For the drawn fibers, values as high as 0.007 were obtained. For annealed drawn fibers, we obtained a value of 0.006.

The value of the Hermans–Stein orientation factor f_c from the WAXS studies reached as high as 0.85 for melt-spun fibers. We obtained a value of f_c of 0.95 for the drawn fibers.

This suggests that the intrinsic birefringence of P4MP1 was about 0.0075.

TABLE III
$2\theta_{obs}$ Angles and *d*-Spacings for Melt-Spun and Cold-Drawn Fibers as a Function of DR

DDR = 10.1, DR = 3		DDR = 90.4, DR = 3	
$2\theta_{obs}$	*d*-spacing	$2\theta_{obs}$	*d*-spacing
9.9	8.93	9.7	9.12
14.2	6.24	13.8	6.42
17.6	5.04	17.0	5.22
19.4	4.58	18.8	4.72
21.9	4.06	21.1	4.21
22.6	3.93	21.9	4.06

θ_{obs} is the observed Bragg angle.

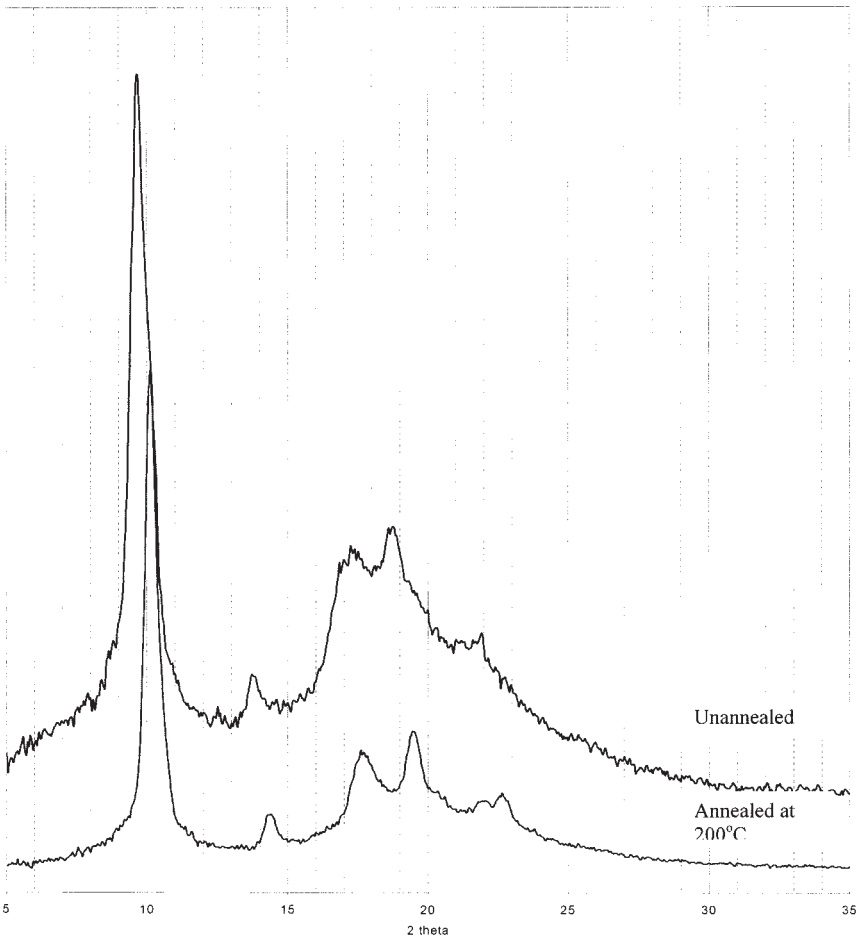

Figure 7 X-ray diffractometer scan of the melt-spun P4MP1 filament, which was cold drawn and annealed (melt-spinning DDR = 90.4, cold-drawing DR = 3).

CONCLUSIONS

The crystal structure and orientation of P4MP1 melt-spun drawn and annealed fibers were investigated. The higher DDR fibers had *d*-spacings closer to the accepted values of form I, a tetragonal unit cell. Cold-drawn fibers had similar values to the melt-spun fibers. The annealing of the cold-drawn fibers produced changes in the unit cell that made it's structure similar to that previously observed by He and Porter.[23]

TABLE IV
$2\theta_{obs}$ Angles and *d*-spacings for Melt-Spun and Annealed Fibers

DDR = 10.1, annealed at 200°C (1 h)		DDR = 90.4, annealed at 200°C (1 h)	
$2\theta_{obs}$	*d*-spacing	$2\theta_{obs}$	*d*-spacing
9.9	8.93	10.1	8.76
13.9	6.37	14.3	6.20
17.0	5.22	17.4	5.10
18.8	4.72	19.4	4.58
21.2	4.19	21.8	4.08
21.9	4.06	22.5	3.95

θ_{obs} is the observed Bragg angle.

TABLE V
$2\theta_{obs}$ Angles and *d*-spacings for Melt-Spun, Cold-Drawn, and Annealed Fibers as a Function of DR

DDR = 90.4, DR = 1, annealed at 200°C (1 h)		DDR = 90.4, DR = 3, annealed at 200°C (1 h)	
$2\theta_{obs}$	*d*-spacing	$2\theta_{obs}$	*d*-spacing
10.1	8.76	10.2	8.67
14.3	6.20	14.4	6.15
17.4	5.10	17.7	5.01
19.4	4.58	19.5	4.55
21.8	4.08	21.9	4.06
22.5	3.95	22.6	3.93

θ_{obs} is the observed Bragg angle.

TABLE VI
Lattice Spacing of P4MP1 with DDRs of 10.1 and 90.4

Miller index	Lattice d-spacing (Å)				
	d_{obs} (DDR = 10.1)	d_{obs} (DDR = 90.4)	d_{calc} Frank et al[11]	d_{calc} Litt[12]	d_{calc} Kusanagi et al.[13]
200	8.93	9.12	9.3	9.25	9.33
220	6.24	6.42	6.6	6.54	6.59
311/212	5.04	5.22	5.42/5.31	—	5.41/5.28
321	4.58	4.72	—	—	—
113/411	4.06	4.21	—	—	4.30/4.29
420/322/203	3.93	4.06	—	4.14	4.17/4.12/4.09

d_{obs} = observed d-spacings, measured from the WAXS pattern.
d_{calc} = calculated d-spacing.

TABLE VII
Lattice Spacing of P4MP1 with a DDR of 90.4 and a DR of 3 annealed for 1 h at 200°C

Miller index	$2\theta_{obs}$	Lattice d-spacing (Å)	
		d_{obs}	d_{calc}
200	10.2	8.67	8.85
210	14.4	6.15	6.26
202	17.7	5.01	5.06
301	—	—	5.32
311	19.5	4.55	4.56
401	21.9	4.06	4.16
220	22.6	3.93	3.96
203	—	—	3.73

d_{calc} = calculated d-spacings with a = 17.70 Å, and b = 8.85 Å, and c = 12.33 Å (orthorhombic: He and Porter[23]).
θ_{obs} is the observed Bragg angle.

References

1. Natta, G.; Pino, P.; Mazzanti, G.; Corradini, P.; Giannini, U. Rend Accad Naz Lincei 1955, 19, 397.
2. Natta, G.; Corradini, P.; Bassi, I. W. Rend Accad Naz Lincei 1955, 19, 404.
3. Day, M. R. Plast Polym 1968, 101.
4. Owen, T. W.; Hull, D. Polymer 1973, 14, 476.
5. Owen, T. W.; Hull, D. Plast Polym 1974, 19.
6. Noether, H. D.; Whitney, W. Kolloid Z Z Polym 1973, 251, 991.
7. Choi, C. H.; White, J. L. Int Polym Process 1998, 13, 78.
8. Johnson, M. B.; Wilkes, G. L. J Plast Film Sheet 2001, 17, 95.
9. Johnson, M. B.; Wilkes, G. L. J Appl Polym Sci 2002, 83, 2095.
10. Bowman, J.; Harriss, N.; Bevis, M. J Mater Sci 1975, 10, 63.
11. Frank, F. C.; Keller, A.; O'Connor, A. Philos Mag 1959, 4, 200.
12. Litt, M. J Polym Sci Part A: Gen Pap 1963, 1, 2219.
13. Kusanagi, H.; Takase, M.; Chatani, Y.; Tadokoro, H. J Polym Sci Polym Phys Ed 1978, 16, 131.
14. Tanda, Y.; Imada, K.; Takayanagi, M. Kogyo Kagaku Zasshi 1966, 69, 1971.
15. Takayanagi, M.; Kawasaki, N. J Macromol Sci Phys 1967, 1, 741.
16. DeRosa, C. Macromolecules 2003, 36, 6087.
17. Nakajima, A.; Hayashi, S.; Taka, T.; Utsumi, N. Kolloid Z Z Polym 1969, 234, 1097.
18. Charlet, G.; Delmas, G. Polym Bull 1982, 6, 367.
19. Charlet, G.; Delmas, G.; Revol, J. F.; Manley, R. S. J. Polymer 1984, 25, 1613.
20. Charlet, G.; Delmas, G. Polymer 1984, 25, 1619.
21. DeRosa, C.; Borriello, A.; Venditto, V.; Corradini, P. Macromolecules 1994, 27, 3864.
22. DeRosa, C. Macromolecules 1999, 32, 935.
23. He, T.; Porter, R. S. Polymer 1987, 28, 1321.
24. Woodward, A. E. Polymer 1964, 5, 293.
25. Inoue, M. Polym Lett 1963, 1, 217.
26. Saunders, F. L. Polym Lett 1964, 2, 755.
27. Stein, R. S. J Polym Sci 1958, 31, 327.